Proceedings of the Seventh International Conference on
Railway Technology: Research, Development and Maintenance
Edited by: J. Pombo
Civil-Comp Conferences, Volume 15, Paper 23.2
Civil-Comp Press, Edinburgh, United Kingdom, 2026
ISSN: 2753-3239, doi: 10.4203/ccc.15.23.2

COOPS: A Synchronised Co-Simulation Framework for Integrated Traffic and DC Traction Power Simulation

Q. Peng, Z. Tian, X. Lyu and X. Liu

University of Birmingham, United Kingdom

Abstract

A synchronised co-simulation is presented that couples train motion, traffic management and traction power flow under a single simulation clock, with power-flow results fed back at every step to constrain train power commands. It enables consistent assessment of timetable decisions together with voltage-limit compliance, regenerative receptivity and substation peak demand in one workflow. The implementation is modular and reproducible, supporting mixed-service operation and allowing performance indicators to be extracted on both train and substation sides without post hoc decoupling. Benchmarking against BS EN 50641 shows close agreement in operational patterns and in voltage and current envelope indicators, establishing a validated baseline for further alignment of energy accounting and for extension to other electrification settings.

Keywords: electrified railways, co-simulation, traction power system, DC power flow, traffic-power interaction, benchmark validation, energy efficiency

1 Introduction

Railways are widely recognised as one of the most energy-efficient forms of land transport, with greenhouse-gas emissions far below those of road and aviation. However, as network expands, the increase in service frequency, the rise in train speed, and the continuous growth in railway power demand not only contribute to the overall energy utilization but also expose the limitations of the traditional traction power system. To enhance sustainability, the UK has set a 2050 net-zero target [1], and international bodies such as the IEA [2] and UIC [3] have proposed energy-saving and emissions-reduction pathways aligned with the Paris Agreement. Many countries and regions now embed transport-efficiency R&D into their net-zero strategies, promoting work on operational optimisation, regenerative braking, and power-supply design. Against net-zero targets and system-level decarbonisation agendas, high-fidelity co-simulation provides a practical means to evaluate operational and infrastructure strategies by synchronising train movement and power-flow behaviour.

This paper presents the Connected and Coordinated Train Operation and Traction Power Supply Systems (COOPS) framework, a digital-twin-oriented co-simulation platform that synchronises single-train dynamics, multi-train traffic management, and DC traction power flow under a unified simulation clock.

Research on railway energy efficiency spans vehicle dynamics, traffic operations, traction power systems, and emerging co-simulation; the following review summarises key advances and highlights the gaps that motivate an integrated COOPS framework.

Existing railway energy efficiency research encompasses areas such as optimising individual train trajectories, traffic control, and modelling traction power systems. However, these research directions frequently employ simplified cross-domain interaction models for evaluation. Single-train optimal control and real-time capable advisory algorithms have achieved robust energy-efficient trajectories for high-speed and metro contexts [4,5,6], yet they typically simplify traction-network effects and multi-train electrical interactions [7]. At the network level, advanced traffic management and signalling (including moving-block concepts) improve capacity and punctuality by tightening the coupling between trajectory advice and movement authority [8,9], but electrical constraints and power-supply limits are rarely embedded explicitly within the operational control loop [8]. In parallel, traction power studies highlight receptivity and voltage-compliance limitations in traditional low-voltage DC architectures and motivate assessment frameworks that jointly quantify voltage compliance, energy flows, and peak power evolution on a fully synchronised time basis [10,11]. DC traction networks are typically represented as longitudinal discretised systems, wherein substations and trains serve as dynamic node injection points. This facilitates system-level metric evaluation and enables integration into modular simulation pipelines [11,12].

Prior to the digital twin paradigm, monolithic DC system-energy simulators had already achieved tight coupling between train motion and traction-network solvers. However, such implementations are less suited to multi-rate subsystem integration, real-time data assimilation, operational constraints, and human-in-the-loop supervision. The digital twin concept therefore provides a cyber-physical framework for integrating models, real-time data and control [13], and traction-power roadmaps emphasise asset modelling, real-time constraints, and operator-centric requirements [14]. Distributed co-simulation frameworks provide the temporal synchronisation needed to couple heterogeneous subsystems such as train dynamics, traffic execution, and power flow rigorously [15].

Due to the fact that decoupling or unidirectional simulation may lead to deviations in the prediction of energy consumption, peak demand, regeneration rate and voltage compliance, and the trade-offs of feasibility - efficiency - punctuality rate are rarely quantified on a fully synchronous time basis, it is necessary to build a scalable platform: This platform needs to provide real-time feedback on power grid constraints to adjust the train's running trajectory and support an evaluation system based on standardized indicators. Based on these gaps, the COOPS system proposes a synchronized modular workflow that couples train operations, traffic execution, and DC traction power flow under a unified clock. It establishes a grid-aware mechanism and employs benchmark verification methods to achieve rigorous, reproducible performance quantification under multi-train timetable conditions.

The remainder of this paper is structured as follows: Section 2 introduces the methodology and coupling mechanisms, Section 3 reports results under standardised scenarios, and Section 4 summarises key findings and implications.

2 Methods

This section provides an overview of the COOPS approach and details the implementation of the joint simulation framework and its core modules.

2.1 COOPS Framework

COOPS is a co-simulation environment designed to synchronise operational and electrical behaviour for multiple trains in an electrified railway network. Three functional modules as shown in Figure 1: the Running Train Module (RTM), which simulates traction/braking dynamics and motion control for each train; the Traffic Management Module (TMM), which executes timetables and signalling logic while coordinating multi-train interactions; and the Power Network Module (PNM), which solves DC traction power flows under time-varying traction and regenerative loading.

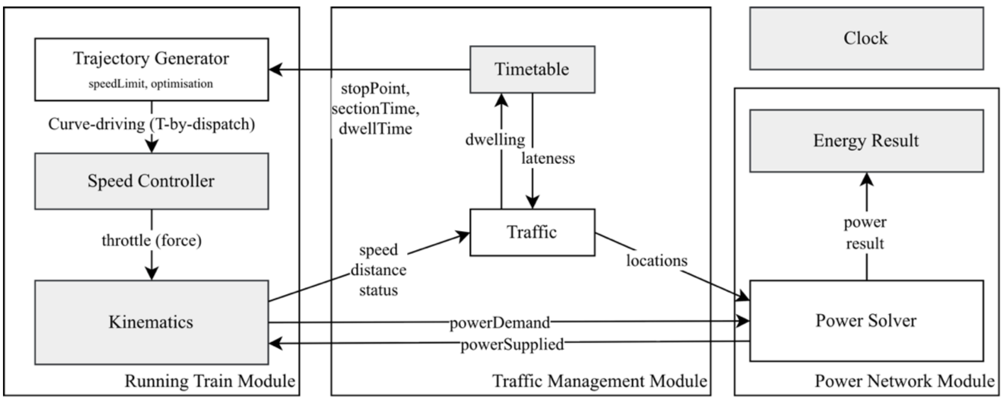

Figure: 1 Framework of the COOPS System.

The framework operates under a unified simulation clock. Within each time step, TMM updates train operational status based on timetable and traffic constraints; RTM calculates instantaneous traction/regenerative power requirements through motion control; while PNM solves corresponding power flows, outputting node voltages and supply feasibility limits. This stepwise interaction mechanism ensures the train's dynamic characteristics consistently comply with grid feasibility requirements while maintaining temporal synchronisation between operational decisions and power network responses.

2.2 Running Train Module

RTM is a single-train simulation engine in COOPS. It has kinematics, trajectory generation, and speed control to produce each train’s trajectory and instantaneous traction and braking demand. It supplies the power requests to PNM and operational status updates to TMM.

2.2.1 Kinematics and Trajectory Generation

The longitudinal motion of each train follows Lomonosov's equation, which is based on Newton's laws of motion and is given by equation (1):

$$\boldsymbol{M}(1+\lambda)\frac{dv}{dt} = \boldsymbol{F}_{t/b}(u,v) - \boldsymbol{w}(v) - \boldsymbol{F}_g(s) \tag{1}$$

where $\boldsymbol{M}$ is the train mass; λ is the rotary inertia factor, and $\boldsymbol{F}_{t/b}$ represents the traction or braking force controlled by the throttle $\boldsymbol{u} \in [-1,1]$. The basic running resistance follows the Davis equation $\boldsymbol{w}(v) = \boldsymbol{A} + \boldsymbol{B}v + \boldsymbol{C}v^2$, and $\boldsymbol{F}_g(s)$ denotes the gradient resistance derived from the track profile grades.

Prior to real-time simulation, a feasible reference speed profile $\boldsymbol{v}^*(\boldsymbol{s})$ is pre-calculated. This process integrates the motion equations under constraints of line geometry, speed limits, and maximum traction/braking characteristics. By combining the traction-limited and braking-limited envelopes, a time-distance-speed dataset (t,s,v) is generated, serving as the target trajectory for online control.

2.2.2 Speed control

During each simulation step, the RTM receives commands from the TMM and calculates the target speed through interpolation against the reference curve. The PID controller computes the required throttle/brake commands to track the target speed. These commands are converted into mechanical power demands, which are then transformed into electrical power requirements and transmitted to the PNM. Should the PNM return constrained power supply capabilities, the actual traction/braking force exerted by the RTM is correspondingly limited.

2.3 Traffic Management Module

TMM is the supervisory unit that orchestrates multi-train operations, timetable execution, and signalling, and coordinates information exchange between RTM and PNM. It controls the analogue sequence and ensures that operational decisions remain consistent with instantaneous power supply constraint.

2.3.1 Traffic Generation and Dispatching

The T is the set of all scheduled services defined in the timetable. For a specific service $i \in \mathrm{T}$, its activation status is determined by comparing the current simulation clock t against its scheduled departure time t_i^{dep} and arrival time t_i^{arr} given by equation (2):

$$Status_{i(t)} = \begin{cases} Active, \text{ if } t \geq t_i^{dep} \wedge t < t_i^{arr} \\ Inactive, \ otherwise \end{cases} \tag{2}$$

At each simulation tick, the TMM scans the schedule and updates the set of currently active trains $\mathrm{A}(t)$ by instantiating any service that transitions to the '*Active*' state given by equation (3):

$$\mathrm{A}(t) = \{ i \in \mathrm{T} \mid Status_i(t) = Active \} \tag{3}$$

When active, the TMM updates the train's state (s_i, v_i) at every time step, synchronising its progress against the traffic timetable.

2.3.2 Power-Flow Interface and Load Aggregation

A key function of TMM is to couple the discrete logic of train operations with the continuous physical characteristics of the power supply network. At each time step, the TMM aggregates the instantaneous states of all $\boldsymbol{N}(t) = |\mathrm{A}(t)|$ active trains into a system-wide state snapshot $\boldsymbol{X}(t)$ given by equation (4):

$$\boldsymbol{X}(t) = \{ (\boldsymbol{s}_i(t), \boldsymbol{P}_{req,i}(t), \boldsymbol{d}_i(t)) \mid i \in \mathrm{A}(t) \} \tag{4}$$

where $\boldsymbol{s}_i$ is the position, $\boldsymbol{P}_{req,i}$ is the power demand requested by the RTM, and $\boldsymbol{d}_i$ indicates direction.

This combined load vector is transmitted to PNM. Upon solving the load flow, the PNM returns a supply capability vector $\boldsymbol{P}_{sup}(t)$. TMM then enforces network consistency by clipping the final permissible power for each train i by equation (5):

$$\boldsymbol{P}_{final,i}(t) = \min(\boldsymbol{P}_{req,i}(t), \boldsymbol{P}_{sup,i}(t)) \tag{5}$$

This mechanism ensures that the execution of operations is strictly constrained by the instantaneous capacity of the power supply system.

2.4 Power Network Module

PNM performs physically based DC traction power flow calculations based on the train's position over time and the power demand from TMM. It constructs a three-conductor admittance model, assembles current injections for trains and substations, solves nodal voltages, and feeds back voltages and available supply capacity to TMM and RTM.

2.4.1 Power network solver

Because trains behave approximately as constant-power devices within their normal voltage range, the relationship between nodal voltages and train current injections is nonlinear. PNM therefore employs an iterative current-injection solution: nodal voltages are initialised using the previously converged solution to accelerate convergence, then train current injections are updated based on terminal voltage, and the linear network equations are solved repeatedly until convergence criteria are met.

2.4.2 Iterative Solver and Mode Switching

Since trains typically operate as constant-power loads ($\boldsymbol{P}=\boldsymbol{V}\cdot\boldsymbol{I}$) within their normal voltage range, the interaction between nodal voltages and current injections is non-linear. As illustrated in the Figure 2, the PNM employs an iterative current injection method based on fixed-point iteration to solve the network equations.

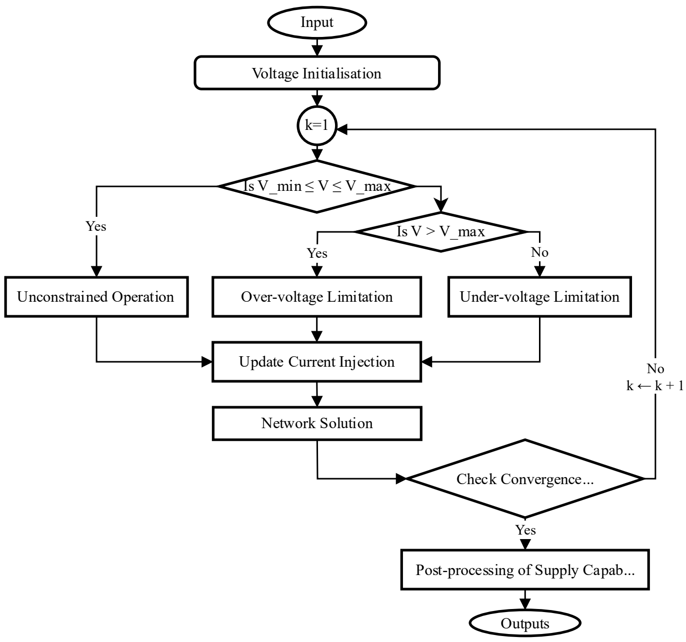

Figure 2: Flowchart of the iterative current injection solver

The solution process begins by initialising the nodal voltage vector $\boldsymbol{V}^{(0)}$ using a strategy, inheriting the converged solution from the previous time step ($t-\Delta t$) to accelerate convergence. The algorithm then enters an iterative loop where the equivalent current injection $\boldsymbol{I}_i^{(k)}$ for each train i is updated based on its terminal voltage $V_i^{(k-1)}$. Crucially, the solver evaluates the operational mode of each train against network protection thresholds ($V_{\max}^{regen}$, $V_{\min}^{trac}$) at every iteration.

This mode-dependent current injection is defined by the equation (6):

$$I_i^{(k)} = \begin{cases} \dfrac{P_{req,i}}{V_i^{(k-1)}} & \left(V_{\min}^{trac} \le V_i^{(k-1)} \le V_{\max}^{regen}\right) \\ -\dfrac{V_i^{(k-1)} - V_{\max}^{\text{limit}}}{R_{regen}} & \left(V_i^{(k-1)} > V_{\max}^{regen} \text{ and } P_{req,i} < 0\right) \\ \dfrac{V_i^{(k-1)} - V_{\min}^{\text{limit}}}{R_{under}} & \left(V_i^{(k-1)} < V_{\min}^{trac} \text{ and } P_{req,i} > 0\right) \end{cases} \tag{6}$$

In the Normal Mode, the train acts as an ideal constant power load. However, if the grid cannot absorb regenerative energy (Over-voltage Mode), the train effectively switches to a dynamic braking resistor model (R_{regen}), limiting the injected current to maintain the voltage at the safety limit. Similarly, under critical voltage sag (Under-voltage Mode), the train switches to an equivalent impedance (R_{under}) to reduce its power draw and prevent network collapse.

With the updated injection vector $I^{(k)}$, the linear network equations are solved via sparse matrix factorization ($V^{(k)} = Y^{-1} I^{(k)}$). This cycle repeats until the maximum power mismatch across all train nodes falls below a prescribed tolerance ň (e.g., 10 W). Upon convergence, the final feasible power states are extracted to compute the supply capacity P_{sup} for system.

2.4.3 Supply Capacity Indicator

A key contribution of the COOPS framework lies in its derivation and calculation of energy supply (P_{sup}) from the converged power flow solution. Unlike traditional tools that merely report violations, the PNM quantifies the maximum power the network could support at that specific moment. Upon convergence, the available supply capacity $P_{sup,i}$ for each train is calculated based on its final operating state (7):

$$P_{(\sup,i)(t)} = \begin{cases} \left| I_i^{final} \cdot V_i^{final} \right| & \text{limiting mode} \\ P_{(req,i)(t)} & \text{normal operation} \end{cases} \tag{7}$$

This value is fed back to the TMM and RTM. The operational module ensures network consistency by reducing the working power of trains in the current phase: $P_{final,i}(t) = \min\left(\left|P_{req,i}(t)\right|, P_{\sup,i}(t)\right)$.

3 Results and Validation

This section reports the benchmarking results against the standard data, covering both kinematic and electrical verification.

3.1 Experimental Setup and Benchmarking

To verify the accuracy and computational performance of the proposed COOPS framework, the paper conducted a comprehensive verification using the defined standardized test cases of BS EN 50641:2020[16]. This standard provides a strict benchmark for verifying railway simulation tools by specifying precise infrastructure parameters, train characteristics and timetables, along with a set of BSI standard data. In this article, if the COOPS value is within the corresponding range, it is regarded as the indicator meeting the requirements. When the value exceeds the range, the deviation will be calculated based on the nearest boundary.

The selected case study simulates a DC 1.5kV traction network, which is a 50 km line powered by 7 substations. The traffic model consists of 6 train services including High-Speed (HS), Suburban (SUB), and Freight (FR) trains, operating under a mixed-traffic timetable. All infrastructure parameters, including gradient profiles, speed limits, and line impedances, are configured in strict accordance with the BSI benchmark specifications.

The complete traffic diagram generated by COOPS is presented in Figure 3. This timetable plots the spatio-temporal trajectories of all departing trains, where the slope of each curve corresponds to the instantaneous speed controlled by the RTM.

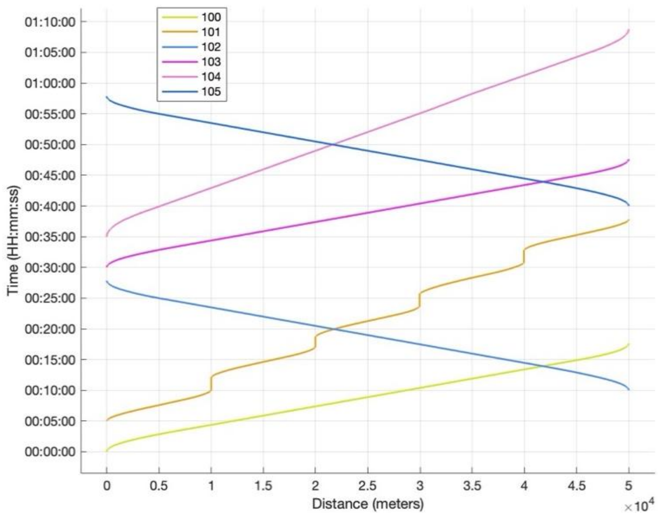

Figure 3: Simulated timetable traffic diagram

3.2 RTM Verification

To validate the kinematic accuracy of the RTM, the paper compares the running time of the line section with standard data and assesses it based on overrun conditions relative to the nearest boundary.

Table 1 shows that the suburban service (Train 101) falls within the prescribed interval, indicating consistent implementation of station events and state transitions under frequent start–stop operation. In contrast, the HS and FR services show small positive exceedances.

.

Train ID	Type	BSI Data (s)	COOPS Results (s)
100	HS	1026-1046	1054.6 (+0.83%)
101	SUB	1958-1978	1971
102	HS	1018-1038	1061 (+2.2%)
103	HS	1026-1046	1054.6 (+0.83%)
104	FR	1954-1974	2005 (+1.6%)
105	HS	1018-1038	1061 (+2.2%)

Table 1: Travelling-time verification against the standard data.

Nevertheless, Figure 4 shows the speed-distance curve still aligns with expected operational patterns at the physical level, high-speed trains exhibit acceleration-cruise-braking characteristics, metro trains show periodic start-stop arcs, while express trains display low-speed plateau phases, indicating stable trajectory tracking without numerical oscillations. These results validate the operational logic while revealing that the current control and dynamics parameterisation scheme provides conservative running time estimates for trains under the “minimum run-time” benchmark setting.

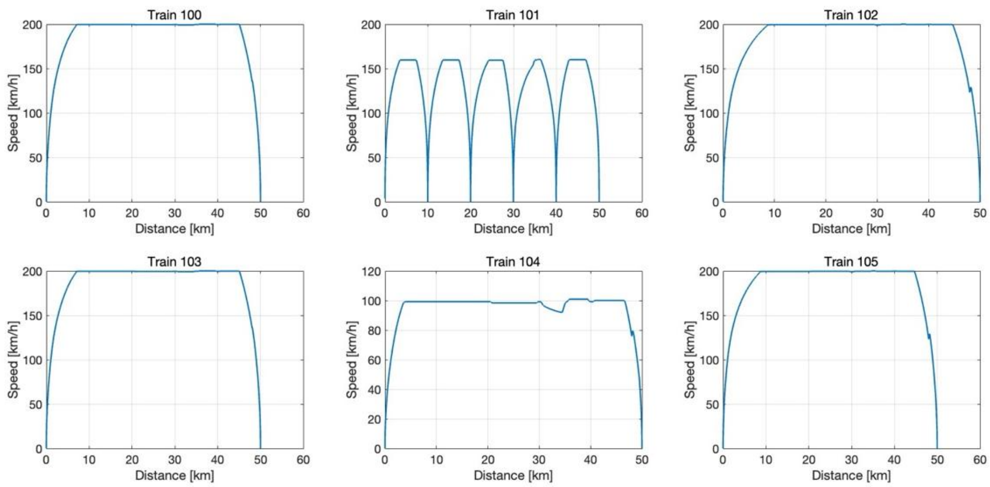

Figure 4: Speed–distance curves for the six services.

3.3 PNM Verification

The electrical validation assesses the accuracy of the DC power-flow solution and the voltage-dependent train electrical models under a synchronised time-step. Comparative indicators are categorised into two types: electrical parameters on the train side and load statistics on the substation side.

3.3.1 Train Voltage and Energy Performance

Table 2 compares train-side voltage and energy metrics against standard data. The maximum pantograph voltage for all simulated trains closely matched the reference values, remaining within specified tolerances and accurately reproducing the overvoltage threshold near 1.95 kV. The average effective voltage also exhibited minimal deviation, indicating high-precision capture of operational levels and power-sharing behaviour within the network. Regarding minimum voltage, four out of six trains met tolerance requirements, while SUB (ID: 101) and one HS (ID: 103) exceeded tolerance limits.

ID	V_min (V)		V_max (V)		V_mean_useful (V)		Energy Consumed (kWh)	
	BSI	COOPS	BSI	COOPS	BSI	COOPS	BSI	COOPS
100	1137 - 1287	1146.9	1867-2017	1946.4	1486 - 1546	1534.1	1334 - 1394	1307.53 (-1.9%)
101	1249 - 1399	1173.5 (-5.7%)	1875-2025	1944.8	1604 - 1664	1593.3	1163 - 1223	1230.1 (+0.6%)
102	1165 - 1315	1289.8	1866-2016	1947.3	1565 - 1625	1575.5	1333 - 1393	1296.53 (-2.7%)
103	1136 - 1286	1353.6 (+5.6%)	1859-2009	1949.8	1486 - 1546	1532.9	1334 - 1394	1264.2 (-5.1%)
104	1208 - 1358	1273.4	1875-2025	1945.5	1546 - 1606	1604.5	1443 - 1503	1450.1
105	1162 - 1312	1180.1	1862-2002	1940.2	1559 - 1619	1615.8	1333 - 1393	1322.6

Table 2: Power results of train side verification against the standard data.

3.3.2 Substation Loading and Supply Capability

As shown in Table 3, substation-side metrics were benchmarked against the BS EN 50641 frequency band. The instantaneous and one-minute peak current values were accurate and exhibited a reasonable spatial distribution across substations, with most readings falling within or near the reference frequency band. Deviations were concentrated in a few feeder sections. The central substation recorded the highest demand, while downstream substations demonstrated comparable demand levels. Certain upstream substations simultaneously underestimated both instantaneous and one-minute peak currents, while another substation compensated by overestimating, indicating a redistribution of supply contributions. Substation energy contributions exhibited an overall consistent pattern across the network. However, estimation deviations exceeded tolerance limits at certain substations, with some exhibiting systematic underestimation of energy supply.

ID	I_max_Inst (A)		I_max_1min (A)		Supplied Energy (kWh)	
	BSI	COOPS	BSI	COOPS	BSI	COOPS
1	5201-5501	4904.4 (-5.5%)	4710-4910	4615.5 (-2.0%)	1299-1499	1121.8 (-12.6%)
2	4177-4477	4002.1 (-4.0%)	3705-3905	3205.2 (-13.1%)	1281-1481	1235 (-3.3%)
3	2238-2538	2698.8 (+6.7%)	2017-2217	2118.8	733-933	803.54
4	5250-5550	5101.5 (-2.8%)	4661-4861	4574.2 (-1.8%)	2140-2340	2156.4
5	5310-5610	5493.4	4618-4818	4730.6	2143-2343	1973.3 (-7.5%)
6	4739-5039	4931.7	4438-4638	4618.9	806-1006	894.9
7	4208-4508	4398.7	3751-3951	3780.6	414-614	540.6

Table 3: Power results of substation side verification against the standard data.

4 Conclusions and Contributions

This section summarises the main findings and discusses the practical implications of the proposed framework, together with directions for further improvement.

4.1 Running Time Deviation and Calibration Priority

Although the RTM system can replicate benchmark suburban station services with negligible running time deviations, high-speed trains and freight services consistently lag behind the standard data. We decompose the journey into acceleration, cruising, and braking phases, comparing durations and key transition points against benchmark assumptions. This interpretation aligns with standard data, where minor deviations typically stem from undisclosed track profile variations—addressable through targeted calibration rather than structural changes to the simulation framework.

Consequently, residual travel time discrepancies are more likely attributable to conservative control and dynamic parameterizesation than to timetable or event logic errors. Typical influencing factors include actuator saturation, rate limiting, or filtering within traction/braking commands, resulting in smoother acceleration and braking transients; minor variations in traction/braking capability, resistance parameters, or gradient discretisation accumulate during extended cruising and gradient sections; discrete time event triggers and stop criteria may introduce slightly conservative braking initiation. Following the benchmark priority validation principle, the next step is to calibrate RTM parameters and control settings to return travel time to the BSI band while maintaining stability and correct qualitative trajectory shape.

4.2 The systematic underestimation of supplied energy

Benchmark test results indicate a systematic underestimation of substation power supply capacity, despite the overall magnitude of peak current metrics being correct and exhibiting a reasonable spatial distribution. Train-side voltages align substantially with standard data. The observed energy deviations are not inconsistent with the voltage–current envelope agreement, because the benchmark "supplied energy" is highly sensitive to metering boundaries and to the discrete-time integration and logging chain. Therefore, the immediate objective is to enforce boundary-consistent energy accounting before claiming full energy fidelity.

The combined results above demonstrate that the methodology employed in this paper operates within a credible physical framework. Its network topology, power supply zone delineation, and train-substation mapping all conform to standards and maintain fundamental accuracy. Consequently, the primary cause of the power supply energy shortfall is more likely attributable to inconsistencies in the energy metering boundaries and issues with the discrete-time integration and recording process, rather than structural flaws within the power model itself. In practical application, 'power supply energy' is highly sensitive to boundary definitions: if standard reference values accurately reflect boundary energy encompassing converter/rectifier losses, line losses, or auxiliary power consumption, while the current implementation integrates power at DC bus injection points, this may generate systematic negative deviations. In the traction regeneration hybrid operation mode, the peak current remains basically unchanged, but the cumulative energy value may change significantly, which may amplify the data deviation. In addition, discrete-time integration is vulnerable to sampling omissions and signal mismatches. For instance, sampling loss during mode conversion, the failure of the post-processing power signal integration to fully align with the converging solution, or the application of smoothing/truncation processing before accumulation may all reduce the energy supply value after integration, while the instantaneous current remains basically unchanged. The crux lies in the rationality of energy distribution between substations. The verification of higher benchmark frequency bands corresponding to high-energy-consumption substations within the thesis model confirms the accuracy of energy partitioning. This indicates residual errors are concentrated in cumulative metering rather than spatial allocation or the logical construction of physical models. The next step requires achieving directional energy balance closure under unified rules, ultimately adjusting the sum of all integrals within numerical tolerance limits.

4.3 Summary of Contributions

Motivated by the limitations of decoupled simulation tools for railway operation and traction power supply, this paper presents COOPS and makes the following contributions:

1. A synchronised, modular co-simulation workflow that couples traffic execution (TMM), train motion (RTM) and DC traction power flow (PNM) with multiple data evaluations for multi-train interactions.
2. Benchmark validation based on BS EN 50641 demonstrates reliability in critical operating modes and electrical envelope metrics, thereby supporting engineering-level assessments of network load and voltage compliance.
3. Establish a reusable foundational framework for systematic benchmark alignment and scaling, incorporating energy balance audits, and achieve the portability of PNM modelling methodologies to other electrification scenarios.

4.4 Future Work

The priority is to further optimise the alignment between COOPS outputs and the benchmark metrics of BS EN 50641. Specific measures include: coordinating train-side and substation-side parameters (encompassing auxiliary loads, efficiency agreements, and network losses) through system performance energy analysis, whilst optimising discrete-time power and energy supply calculations to reduce energy consumption deviation while maintaining stable voltage characteristics. The second critical task involves extending the existing DC traction model to AC electrification systems. This entails integrating transformer and supply section modelling, reactive power effects, and AC power flow calculation processes to support a broader standardised metric framework. Once benchmark accuracy is fully established for both DC and AC scenarios, the COOPS system may expand optional operational layer functionalities. These include grid-aware feedback control, virtual coupling, and scenario-based research for integrated driver assistance features.

Acknowledgements

This work was supported in part by the Engineering and Physical Sciences Research Council (EPSRC) under the project ‘Connected and Coordinated Train Operation and Traction Power Supply Systems (COOPS)’ (Grant No. EP/Y003136/1).

References

[1] Department for Transport, "Decarbonising Transport: A Better, Greener Britain", UK Government, London, United Kingdom, 2021.
[2] International Energy Agency (IEA), International Union of Railways (UIC), "The Future of Rail: Opportunities for Energy and the Environment", IEA, Paris, France, 2019.
[3] International Union of Railways (UIC), "Design a Better Future: Vision of Rail 2030", UIC, Paris, France, 2021.

[4] M. Miyatake, H. Ko, "Optimization of train speed profile for minimum energy consumption", IEEJ Transactions on Electrical and Electronic Engineering, 5, 263-269, 2010.
[5] Z. Tian, N. Zhao, S. Hillmansen, et al., "SmartDrive: Traction energy optimization and applications in rail systems", IEEE Transactions on Intelligent Transportation Systems, 20, 2764-2773, 2019.
[6] Z. Xiao, Q. Wang, P. Sun, et al., "Real-time energy-efficient driver advisory system for high-speed trains", IEEE Transactions on Transportation Electrification, 7, 3163-3172, 2021.
[7] N. Ghaviha, M. Bohlin, C. Holmberg, et al., "A driver advisory system with dynamic losses for passenger electric multiple units", Transportation Research Part C: Emerging Technologies, 85, 111-130, 2017.
[8] N.D. Versluis, E. Quaglietta, R.M.P. Goverde, et al., "Real-time railway traffic management under moving-block signalling: A literature review and research agenda", Transportation Research Part C: Emerging Technologies, 158, 104438, 2024.
[9] H. Song, H. Liu, E. Schnieder, "A train-centric communication-based new movement authority proposal for ETCS-2", IEEE Transactions on Intelligent Transportation Systems, 20, 2328-2338, 2019.
[10] H. Hu, Y. Liu, Y. Li, et al., "Traction power systems for electrified railways: evolution, state of the art, and future trends", Railway Engineering Science, 32, 1-19, 2024.
[11] Z. Tian, "System energy optimisation strategies for DC railway traction power networks", Ph.D. dissertation, University of Birmingham, Birmingham, United Kingdom, 2017.
[12] D. Ciechanowicz, D. Pelzer, B. Bartenschlager, et al., "A modular power system planning and power flow simulation framework for generating and evaluating power network models", IEEE Transactions on Power Systems, 32, 2214-2224, 2017.
[13] S. Ghaboura, R. Ferdousi, F. Laamarti, et al., "Digital twin for railway: A comprehensive survey", IEEE Access, 11, 120237-120257, 2023.
[14] M. Ahmadi, H.J. Kaleybar, M. Brenna, et al., "Adapting digital twin technology in electric railway power systems", in "2021 12th Power Electronics, Drive Systems, and Technologies Conference (PEDSTC)", IEEE, Tabriz, Iran, 1-6, 2021.
[15] T. Pieper, R. Obermaisser, "Distributed co-simulation for software-in-the-loop testing of networked railway systems", in "2018 7th Mediterranean Conference on Embedded Computing (MECO)", IEEE, Budva, Montenegro, 1-5, 2018.
[16] British Standards Institution (BSI), "BS EN 50641:2020: Railway applications - Fixed installations - Requirements for the validation of simulation tools used for the design of electric traction power supply systems", BSI Standards Limited, London, United Kingdom, 2020.